

Implementing quantum Fourier transform using three qubits

Mouhcine Yachi^a, Radouan Hab-arrih^a and Ahmed Jellal^{*a,b}

^a*Laboratory of Theoretical Physics, Faculty of Sciences, Chouaib Doukkali University,
PO Box 20, 24000 El Jadida, Morocco*

^b*Canadian Quantum Research Center, 204-3002 32 Ave Vernon,
BC V1T 2L7, Canada*

Abstract

Using the circulant symmetry of a Hamiltonian describing three qubits, we realize the quantum Fourier transform. This symmetry allows us to construct a set of eigenvectors independently on the magnitude of physical parameters involved in the Hamiltonian and as a result the entanglement will be maintained. The realization will be leaned on trapped ions and the gate implementation requires an adiabatic transition from each spin product state to Fourier modes. The fidelity was numerically calculated and the results show important values. Finally, we discuss the acceleration of the gate by using the counter-driving field.

PACS numbers: 03.65.Fd, 03.65.Ge, 03.65.Ud, 03.67.Hk

Keywords: Three qubits, circulant symmetry, entanglement, quantum Fourier transform, adiabatic transition, counter-driving-field.

*a.jellal@ucd.ac.ma

1 Introduction

Paul Benioff suggested a quantum mechanical model of the Turing machine [1] in 1980, launching a new field of study known as quantum computers (QCs). Richard Feynman demonstrated in 1982 that QCs may be used to mimic complicated systems (living cells, city traffic, the human brain, and the universe, \dots) [2]. Seth Lloyd demonstrated four decades later that the basic units of a QC are an array of nuclear magnetic resonance spins [3]. QC is a device that uses quantum mechanics to process data while maintaining quantum coherence [4]. As a result, QC can tackle the most difficult computational problems that even today's most powerful supercomputers cannot solve [5]. As an example, Shor's quantum algorithm (SQA) for factoring large numbers [6] is the most seminal motivation behind the development of QCs [5]. It is well-known in quantum computing that the physical implementation of SQA requires a gate of particular importance called quantum Fourier transform (QFT) [7]. QFT is the quantum implementation of the discrete Fourier transform over the amplitudes of a wavefunction, which acts on a vector $|x\rangle \in \mathbb{C}^N$ as $|x\rangle \xrightarrow{\text{QFT}} |y\rangle = \frac{1}{\sqrt{N}} \sum_{j=0}^{N-1} e^{2\pi i x j / N} |j\rangle$ [5]. QFT is widely used as a key subroutine in several factoring algorithms like for instance quantum amplitude estimation [8] and quantum counting [9].

The circulant matrices have been thoroughly investigated in [10, 11], and the set of invertible circulant matrices forms a group in terms of matrix multiplication. Geometry, linear coding, and graph theory, all use such matrices, one may see [12–17]. Also for more than 47 years, vibration analysis has focused on systems with circulant symmetry. Many of these contributions were motivated by vibration studies of general rotationally periodic systems [15], bladed disks, planetary gear systems, rings, circular plates, disk spindle systems, centrifugal pendulum vibration absorbers, space antennae, and microelectromechanical system frequency filters.

The circulant Hamiltonians are addressed [18] in terms of the physical implementation of logical QFT, which related to the fact that the eigenspectrum of circulant matrix is spanned by the Fourier modes [10, 19]. Ivanov and Vitanov [20] recently proposed a Hamiltonian based on two spins emerging in a magnetic field, creating Rabi oscillations, and obtained circulant symmetry by modifying the coupling strength of the spin-spin interaction. As a result, they demonstrated that the eigenvectors are independent of the magnitude of the physical parameters, implying entanglement protection, and the resulting system can subsequently be employed as a logical QFT. Wu and his colleagues [21] presented two approaches for implementing quantum phase gates based on adiabatic passing and phase control of the driving fields. They studied the experimental feasibility, gate fidelity and decoherence effect for both schemes. Moreover, the shortcuts to adiabaticity have become instrumental in preparing and driving internal and motional states in atomic, molecular and solid-state physics, for a complete review we refer to [22].

Motivated by the results developed in [20], we study a Hamiltonian describing three spins in a magnetic field, coupled via linear and non-linear interactions. The last coupling generally arises when the interaction medium is non-linear [23–25] and remains an important ingredient in generating a circulant Hamiltonian. To build a logical QFT, we propose two schemes based on the physical parameter choices. The eigenvectors of our circulant Hamiltonian do not depend on the parameters, which protects entanglement during the gate implementation as long as the circulant symmetry is

maintained. We use an energy offset Hamiltonian $H_0(t) = \sum_{j=1}^3 \Delta_j(t)\sigma_j^z$ to break the circulant symmetry during the transition. We adjust the physical parameters and the detuning $\Delta_j(t)$ to realize the circulant symmetry at the end of the transition t_f . We sinusoidally modulate the physical parameters in time to show that it is possible to adiabatically obtain a superposition of the quantum Fourier modes from any initial state with high fidelity. As the adiabatic evolution is robust but still limited by the non-adiabatic transition, we introduce a counter-driving Hamiltonian $H_{CD}(t)$ [26] to suppress these transitions. Under suitable conditions of the physical parameters, we determine the eigenvectors associated with the total Hamiltonian. These allow us to combine our gate with the short-cut to adiabaticity scheme in order to accelerate the gate. Based on the proposal described in [20], we suggest a way to physically implement the gate.

The outlines of our paper are summarized as follows. In Sec. 2, we propose a Hamiltonian describing three qubits with different interactions in addition to Rabi oscillations and show how to obtain the circulant symmetry. The adiabatic transition technique is performed to end up with the Fourier modes in Sec. 3. The physical implementation of the obtained QFT gate will be discussed in Sec. 4. The non-degeneracy of frequencies, the fidelities of our gate and the creation of entangled state will be numerically analyzed by sinusoidally varying the physical parameters in Sec. 5. We discuss the shortcut to adiabaticity scheme combined with our gate in Sec. 6. Finally, we close by concluding our work.

2 Theoretical model

We consider three spins that emerged in a magnetic field to achieve our task, forming a three-qubit gate system as presented in Figure 1.

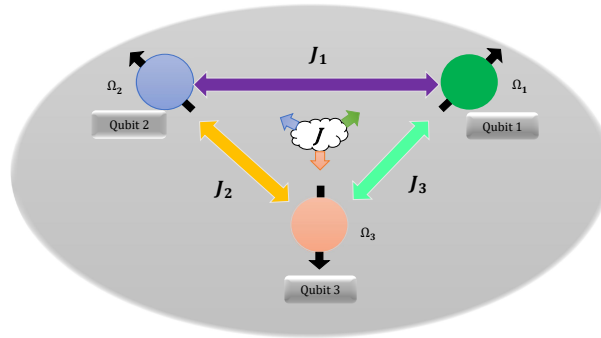


Figure 1 – (color online) The schematic presents the interactions of strengths J_j between three coupled qubits emerging in a magnetic field with the Rabi frequencies Ω_j .

It can be described by a Hamiltonian involving two types of interaction, such as

$$\begin{aligned}
H = & J_1(\sigma_1^+ e^{-i\phi_{12}} + \sigma_1^- e^{i\phi_{12}})(\sigma_2^+ e^{-i\phi_{21}} + \sigma_2^- e^{i\phi_{21}}) + J_2(\sigma_2^+ e^{-i\phi_{23}} + \sigma_2^- e^{i\phi_{23}})(\sigma_3^+ e^{-i\phi_{32}} + \sigma_3^- e^{i\phi_{32}}) \\
& + J_3(\sigma_1^+ e^{-i\phi_{13}} + \sigma_1^- e^{i\phi_{13}})(\sigma_3^+ e^{-i\phi_{31}} + \sigma_3^- e^{i\phi_{31}}) + \Omega_1(\sigma_1^+ e^{i\theta_1} + \sigma_1^- e^{-i\theta_1}) + \Omega_2(\sigma_2^+ e^{i\theta_2} + \sigma_2^- e^{-i\theta_2}) \\
& + \Omega_3(\sigma_3^+ e^{i\theta_3} + \sigma_3^- e^{-i\theta_3}) + J(\sigma_1^+ e^{-i\phi_1} + \sigma_1^- e^{i\phi_1})(\sigma_2^+ e^{-i\phi_2} + \sigma_2^- e^{i\phi_2})(\sigma_3^+ e^{-i\phi_3} + \sigma_3^- e^{i\phi_3}) \quad (1)
\end{aligned}$$

where $\sigma_j^+ = |\uparrow_j\rangle\langle\downarrow_j|$ and $\sigma_j^- = |\downarrow_j\rangle\langle\uparrow_j|$ stand for spin flip operators, $|\uparrow_j\rangle$ and $|\downarrow_j\rangle$ being the qubit states of the j^{th} spin, with $j = 1, 2, 3$. The first term describes the interaction between spins 1 and 2 of phases ϕ_{12} and ϕ_{21} , whereas the second term covers the interaction between spins 2 and 3 of phases ϕ_{23} and ϕ_{32} , and the third term describes the interaction between spins 1 and 3 of phases ϕ_{13} and ϕ_{31} . The terms, including the Rabi frequencies Ω_j , are the single-qubit transitions with phases θ_j . The last term describes the coupling between the three spins with phases ϕ_j [25]. Note that, our Hamiltonian can be considered as a three-qubit generalization of the Ivanov and Vitanov model for two qubits [20], thanks to the trilinear interaction term.

It is convenient for our task to consider the matrix form of the Hamiltonian (1) and then, in the basis $\mathcal{B}_c = \{|\downarrow\downarrow\downarrow\rangle, |\downarrow\downarrow\uparrow\rangle, |\downarrow\uparrow\downarrow\rangle, |\downarrow\uparrow\uparrow\rangle, |\uparrow\downarrow\downarrow\rangle, |\uparrow\downarrow\uparrow\rangle, |\uparrow\uparrow\downarrow\rangle, |\uparrow\uparrow\uparrow\rangle\}$, we have

$$H = \begin{pmatrix} 0 & \Omega_3 e^{i\theta_3} & \Omega_2 e^{i\theta_2} & J_2 e^{-i\xi_1} & \Omega_1 e^{i\theta_1} & J_3 e^{-i\xi_2} & J_1 e^{-i\xi_3} & J e^{-i\xi_7} \\ \Omega_3 e^{-i\theta_3} & 0 & J_2 e^{-i\xi_4} & \Omega_2 e^{i\theta_2} & J_3 e^{-i\xi_5} & \Omega_1 e^{i\theta_1} & J e^{-i\xi_8} & J_1 e^{-i\xi_3} \\ \Omega_2 e^{-i\theta_2} & J_2 e^{i\xi_4} & 0 & \Omega_3 e^{i\theta_3} & J_1 e^{-i\xi_6} & J e^{-i\xi_9} & \Omega_1 e^{i\theta_1} & J_3 e^{-i\xi_2} \\ J_2 e^{i\xi_1} & \Omega_2 e^{-i\theta_2} & \Omega_3 e^{-i\theta_3} & 0 & J e^{-i\xi_{10}} & J_1 e^{-i\xi_6} & J_3 e^{-i\xi_5} & \Omega_1 e^{i\theta_1} \\ \Omega_1 e^{-i\theta_1} & J_3 e^{i\xi_5} & J_1 e^{i\xi_6} & J e^{i\xi_{10}} & 0 & \Omega_3 e^{i\theta_3} & \Omega_2 e^{i\theta_2} & J_2 e^{-i\xi_1} \\ J_3 e^{i\xi_2} & \Omega_1 e^{-i\theta_1} & J e^{i\xi_9} & J_1 e^{i\xi_6} & \Omega_3 e^{-i\theta_3} & 0 & J_2 e^{-i\xi_4} & \Omega_2 e^{i\theta_2} \\ J_1 e^{i\xi_3} & J e^{i\xi_8} & \Omega_1 e^{-i\theta_1} & J_3 e^{i\xi_5} & \Omega_2 e^{-i\theta_2} & J_2 e^{i\xi_4} & 0 & \Omega_3 e^{i\theta_3} \\ J e^{i\xi_7} & J_1 e^{i\xi_3} & J_3 e^{i\xi_2} & \Omega_1 e^{-i\theta_1} & J_2 e^{i\xi_1} & \Omega_2 e^{-i\theta_2} & \Omega_3 e^{-i\theta_3} & 0 \end{pmatrix} \quad (2)$$

where the ten angles $\xi_1 = \phi_{23} + \phi_{32}$, $\xi_2 = \phi_{13} + \phi_{31}$, $\xi_3 = \phi_{12} + \phi_{21}$, $\xi_4 = \phi_{23} - \phi_{32}$, $\xi_5 = \phi_{13} - \phi_{31}$, $\xi_6 = \phi_{12} - \phi_{21}$, $\xi_7 = \phi_1 + \phi_2 + \phi_3$, $\xi_8 = \phi_1 + \phi_2 - \phi_3$, $\xi_9 = \phi_1 - \phi_2 + \phi_3$, $\xi_{10} = \phi_1 - \phi_2 - \phi_3$ have been introduced.

In what follows, we are going to find conditions on the involved parameters to end up with the Hamiltonian (2) as a circulant matrix [10,19]. The benefit of the circulant matrix is that its eigenvectors are the vectors of columns of the discrete quantum Fourier transform, and therefore they do not depend on the elements of the circulant matrix. The eigenvectors of our circulant matrix can be mapped into the spin basis \mathcal{B}_c as

$$|\psi_0\rangle = \frac{1}{2\sqrt{2}}(|\downarrow\downarrow\downarrow\rangle + |\downarrow\downarrow\uparrow\rangle + |\downarrow\uparrow\downarrow\rangle + |\downarrow\uparrow\uparrow\rangle + |\uparrow\downarrow\downarrow\rangle + |\uparrow\downarrow\uparrow\rangle + |\uparrow\uparrow\downarrow\rangle + |\uparrow\uparrow\uparrow\rangle) \quad (3)$$

$$|\psi_1\rangle = \frac{1}{2\sqrt{2}}(|\downarrow\downarrow\downarrow\rangle + \omega |\downarrow\downarrow\uparrow\rangle + i |\downarrow\uparrow\downarrow\rangle + i\omega |\downarrow\uparrow\uparrow\rangle - |\uparrow\downarrow\downarrow\rangle - \omega |\uparrow\downarrow\uparrow\rangle - i |\uparrow\uparrow\downarrow\rangle - i\omega |\uparrow\uparrow\uparrow\rangle) \quad (4)$$

$$|\psi_2\rangle = \frac{1}{2\sqrt{2}}(|\downarrow\downarrow\downarrow\rangle + i |\downarrow\downarrow\uparrow\rangle - |\downarrow\uparrow\downarrow\rangle - i |\downarrow\uparrow\uparrow\rangle + |\uparrow\downarrow\downarrow\rangle + i |\uparrow\downarrow\uparrow\rangle - |\uparrow\uparrow\downarrow\rangle - i |\uparrow\uparrow\uparrow\rangle) \quad (5)$$

$$|\psi_3\rangle = \frac{1}{2\sqrt{2}}(|\downarrow\downarrow\downarrow\rangle + i\omega |\downarrow\downarrow\uparrow\rangle - i |\downarrow\uparrow\downarrow\rangle + \omega |\downarrow\uparrow\uparrow\rangle - |\uparrow\downarrow\downarrow\rangle - i\omega |\uparrow\downarrow\uparrow\rangle + i |\uparrow\uparrow\downarrow\rangle - \omega |\uparrow\uparrow\uparrow\rangle) \quad (6)$$

$$|\psi_4\rangle = \frac{1}{2\sqrt{2}}(|\downarrow\downarrow\downarrow\rangle - |\downarrow\downarrow\uparrow\rangle + |\downarrow\uparrow\downarrow\rangle - |\downarrow\uparrow\uparrow\rangle + |\uparrow\downarrow\downarrow\rangle - |\uparrow\downarrow\uparrow\rangle + |\uparrow\uparrow\downarrow\rangle - |\uparrow\uparrow\uparrow\rangle) \quad (7)$$

$$|\psi_5\rangle = \frac{1}{2\sqrt{2}}(|\downarrow\downarrow\downarrow\rangle - \omega |\downarrow\downarrow\uparrow\rangle + i |\downarrow\uparrow\downarrow\rangle - i\omega |\downarrow\uparrow\uparrow\rangle - |\uparrow\downarrow\downarrow\rangle + \omega |\uparrow\downarrow\uparrow\rangle - i |\uparrow\uparrow\downarrow\rangle + i\omega |\uparrow\uparrow\uparrow\rangle) \quad (8)$$

$$|\psi_6\rangle = \frac{1}{2\sqrt{2}}(|\downarrow\downarrow\downarrow\rangle - i |\downarrow\downarrow\uparrow\rangle - |\downarrow\uparrow\downarrow\rangle + i |\downarrow\uparrow\uparrow\rangle + |\uparrow\downarrow\downarrow\rangle - i |\uparrow\downarrow\uparrow\rangle - |\uparrow\uparrow\downarrow\rangle + i |\uparrow\uparrow\uparrow\rangle) \quad (9)$$

$$|\psi_7\rangle = \frac{1}{2\sqrt{2}}(|\downarrow\downarrow\downarrow\rangle - i\omega |\downarrow\downarrow\uparrow\rangle - i |\downarrow\uparrow\downarrow\rangle - \omega |\downarrow\uparrow\uparrow\rangle - |\uparrow\downarrow\downarrow\rangle + i\omega |\uparrow\downarrow\uparrow\rangle + i |\uparrow\uparrow\downarrow\rangle + \omega |\uparrow\uparrow\uparrow\rangle) \quad (10)$$

and we have set the phase factor $\omega = \exp(i\frac{\pi}{4})$. At this point, we show the possibilities that lead to the circulant symmetries. We end up with two scenarios when we require adequate requirements to be met by the physical parameters. Indeed, the first configuration is

$$J_1 = \Omega_2 \quad (11)$$

$$J = J_2 = J_3 = \Omega_3 \quad (12)$$

$$\Omega_1 = 0 \quad (13)$$

$$\theta_2 = \theta_3 = \phi_{32} = \phi_3 = \phi_{21} = -\phi_{31} = \varphi \quad (14)$$

$$\theta_1 = \phi_{23} = \phi_2 = \phi_1 = \phi_{12} = \phi_{13} = 0 \quad (15)$$

which can be injected into (2) to get the first circulant Hamiltonian

$$H_{\text{cir}}^{(1)} = \begin{pmatrix} 0 & Je^{i\varphi} & J_1e^{i\varphi} & Je^{-i\varphi} & 0 & Je^{i\varphi} & J_1e^{-i\varphi} & Je^{-i\varphi} \\ Je^{-i\varphi} & 0 & Je^{i\varphi} & J_1e^{i\varphi} & Je^{-i\varphi} & 0 & Je^{i\varphi} & J_1e^{-i\varphi} \\ J_1e^{-i\varphi} & Je^{-i\varphi} & 0 & Je^{i\varphi} & J_1e^{i\varphi} & Je^{-i\varphi} & 0 & Je^{i\varphi} \\ Je^{i\varphi} & J_1e^{-i\varphi} & Je^{-i\varphi} & 0 & Je^{i\varphi} & J_1e^{i\varphi} & Je^{-i\varphi} & 0 \\ 0 & Je^{i\varphi} & J_1e^{-i\varphi} & Je^{-i\varphi} & 0 & Je^{i\varphi} & J_1e^{i\varphi} & Je^{-i\varphi} \\ Je^{-i\varphi} & 0 & Je^{i\varphi} & J_1e^{-i\varphi} & Je^{-i\varphi} & 0 & Je^{i\varphi} & J_1e^{i\varphi} \\ J_1e^{i\varphi} & Je^{-i\varphi} & 0 & Je^{i\varphi} & J_1e^{-i\varphi} & Je^{-i\varphi} & 0 & Je^{i\varphi} \\ Je^{i\varphi} & J_1e^{i\varphi} & Je^{-i\varphi} & 0 & Je^{i\varphi} & J_1e^{-i\varphi} & Je^{-i\varphi} & 0 \end{pmatrix} \quad (16)$$

whereas the second configuration looks like

$$J_1 = \Omega_2 \quad (17)$$

$$J = J_2 = J_3 = \Omega_3 \quad (18)$$

$$\theta_2 = \theta_3 = \phi_{32} = \phi_3 = \phi_{21} = -\phi_{31} = \varphi \quad (19)$$

$$\theta_1 = \phi_{23} = \phi_2 = \phi_1 = \phi_{12} = \phi_{13} = 0 \quad (20)$$

with $\Omega_1 \neq 0$ and then, from (2) we obtain the second circulant Hamiltonian

$$H_{\text{cir}}^{(2)} = \begin{pmatrix} 0 & Je^{i\varphi} & J_1e^{i\varphi} & Je^{-i\varphi} & \Omega_1 & Je^{i\varphi} & J_1e^{-i\varphi} & Je^{-i\varphi} \\ Je^{-i\varphi} & 0 & Je^{i\varphi} & J_1e^{i\varphi} & Je^{-i\varphi} & \Omega_1 & Je^{i\varphi} & J_1e^{-i\varphi} \\ J_1e^{-i\varphi} & Je^{-i\varphi} & 0 & Je^{i\varphi} & J_1e^{i\varphi} & Je^{-i\varphi} & \Omega_1 & Je^{i\varphi} \\ Je^{i\varphi} & J_1e^{-i\varphi} & Je^{-i\varphi} & 0 & Je^{i\varphi} & J_1e^{i\varphi} & Je^{-i\varphi} & \Omega_1 \\ \Omega_1 & Je^{i\varphi} & J_1e^{-i\varphi} & Je^{-i\varphi} & 0 & Je^{i\varphi} & J_1e^{i\varphi} & Je^{-i\varphi} \\ Je^{-i\varphi} & \Omega_1 & Je^{i\varphi} & J_1e^{-i\varphi} & Je^{-i\varphi} & 0 & Je^{i\varphi} & J_1e^{i\varphi} \\ J_1e^{i\varphi} & Je^{-i\varphi} & \Omega_1 & Je^{i\varphi} & J_1e^{-i\varphi} & Je^{-i\varphi} & 0 & Je^{i\varphi} \\ Je^{i\varphi} & J_1e^{i\varphi} & Je^{-i\varphi} & \Omega_1 & Je^{i\varphi} & J_1e^{-i\varphi} & Je^{-i\varphi} & 0 \end{pmatrix}. \quad (21)$$

At this level, we underline that the presence of the trilinear interaction is necessary to realize the QFT gate. This type of interaction is required to achieve such circulant symmetry. Generalizing to more than three qubits is not trivial because the Hamiltonian will demand multilinear interactions. As a result, discussing the adiabatic transition and shortcut to adiabaticity will be difficult mathematically. In the forthcoming analysis, we focus only on one of the above Hamiltonians, let say $H_{\text{cir}}^{(1)}$, and investigate its basic features.

3 Adiabatic transition to Fourier modes

Some controls can be used to create an adiabatic transition to Fourier modes. Two of these will be discussed here: the energy offset and Rabi frequencies.

3.1 Controlling by energy offset

To realize an adiabatic evolution to the circulant Hamiltonian states (Fourier modes), we add an energy offset $H_0(t)$

$$H_0(t) = \Delta_1(t)\sigma_1^z + \Delta_2(t)\sigma_2^z + \Delta_3(t)\sigma_3^z \quad (22)$$

where the time-dependent detuning $\Delta_j(t)$ of j^{th} spin are necessary to control the adiabatic transition from computational spin states to quantum Fourier states (3-10). Consequently, we have now the Hamiltonian

$$H(t) = H_0(t) + H_{\text{cir}}^{(1)}(t). \quad (23)$$

Remember that in the adiabatic limit, the system is always in the same eigenstates of $H(t)$ [20]. The eigenstates of $H(t)$ will be those of $H_0(t)$ at t_i , and the dynamics will drive them to the Fourier modes at t_f if the couplings and detunings have a specific time dependency. Therefore, adiabatic evolution translates each computational spin state to a Fourier mode, resulting in a single interaction step that generates the QFT. The non-degeneracy between the eigen-frequencies of $H(t)$ must be bigger at any time than the non-adiabatic coupling between each pair of $H(t)$ eigenstates $|\lambda_{\pm}\rangle$, $|\delta_{\pm}\rangle$, $|\mu_{\pm}\rangle$, and $|\gamma_{\pm}\rangle$ of $H(t)$, according to adiabatic evolution. Otherwise, we have the conditions

$$|\mu_{\pm}(t) - \lambda_{\pm}(t)| \gg |\langle \partial_t \mu_{\pm}(t) | \lambda_{\pm}(t) \rangle| \quad (24)$$

$$|\lambda_+(t) - \lambda_-(t)| \gg |\langle \partial_t \lambda_+(t) | \lambda_-(t) \rangle| \quad (25)$$

$$|\lambda_{\pm}(t) - \delta_{\pm}(t)| \gg |\langle \partial_t \lambda_{\pm}(t) | \delta_{\pm}(t) \rangle| \quad (26)$$

$$|\delta_+(t) - \delta_-(t)| \gg |\langle \partial_t \delta_+(t) | \delta_-(t) \rangle| \quad (27)$$

$$|\delta_{\pm}(t) - \gamma_{\pm}(t)| \gg |\langle \partial_t \delta_{\pm}(t) | \gamma_{\pm}(t) \rangle| \quad (28)$$

$$|\gamma_+(t) - \gamma_-(t)| \gg |\langle \partial_t \gamma_+(t) | \gamma_-(t) \rangle|. \quad (29)$$

Let us choose $\varphi = \frac{\pi}{2}$ to simplify our problem, and then we prove in [Appendix A](#) that the eigenvalues $\lambda_{\pm}, \delta_{\pm}, \mu_{\pm}, \gamma_{\pm}$ of the Hamiltonian $H(t)$ (23) are provided by (A.1-A.4). Now, it is worthwhile to mention that the circulant symmetry is broken. We suppose that the system is initially prepared in the computational product states $|\psi_{s_1 s_2 s_3}\rangle = |s_1 s_2 s_3\rangle$ ($s_j = \downarrow_j, \uparrow_j$), which are eigenstates of the Hamiltonian $H_0(t)$. As a result, the initial parameters should verify the conditions

$$\Delta_{1,2,3}(t_i) \gg J(t_i), J_1(t_i) \quad (30)$$

and then $H(t)$ goes to $H_0(t)$. Consequently the eigenvalues become

$$\lambda_{\pm}(t_i) = \pm [\Delta_1(t_i) + \Delta_2(t_i) + \Delta_3(t_i)] \quad (31)$$

$$\delta_{\pm}(t_i) = \pm [\Delta_1(t_i) + \Delta_2(t_i) - \Delta_3(t_i)] \quad (32)$$

$$\mu_{\pm}(t_i) = \pm [\Delta_1(t_i) - \Delta_2(t_i) + \Delta_3(t_i)] \quad (33)$$

$$\gamma_{\pm}(t_i) = \pm [\Delta_1(t_i) - \Delta_2(t_i) - \Delta_3(t_i)] \quad (34)$$

and the $H(t)$ eigenvectors are exactly the computational spin states, i.e. $|\psi(t_i)\rangle = |s_1 s_2 s_3\rangle$,

$$|\lambda_+\rangle = |\downarrow\downarrow\downarrow\rangle, \quad |\lambda_-\rangle = |\uparrow\uparrow\uparrow\rangle \quad (35)$$

$$|\delta_+\rangle = |\downarrow\downarrow\uparrow\rangle, \quad |\delta_-\rangle = |\uparrow\uparrow\downarrow\rangle \quad (36)$$

$$|\mu_+\rangle = |\downarrow\uparrow\downarrow\rangle, \quad |\mu_-\rangle = |\uparrow\downarrow\uparrow\rangle \quad (37)$$

$$|\gamma_+\rangle = |\downarrow\uparrow\uparrow\rangle, \quad |\gamma_-\rangle = |\uparrow\downarrow\downarrow\rangle. \quad (38)$$

To avoid degeneracy, the condition $\Delta_i(t_i) \neq \Delta_j(t_i)$ with $i, j = 1, 2, 3$, and we can have equidistant eigen-frequencies by requiring $\Delta_1(t_i) = 2\Delta_2(t_i) = 4\Delta_3(t_i)$. Furthermore, to obtain the Fourier modes at the final time t_f of transition, the coupling parameters together with detunings should verify the conditions

$$\Delta_{1,2,3}(t_f) \ll J(t_f), J_1(t_f). \quad (39)$$

As a result, the total Hamiltonian evolves to a circulant one, i.e. $H(t) \rightarrow H_{\text{cir}}^{(1)}(t)$, and its eigenspectrum becomes that of $H_{\text{cir}}^{(1)}(t)$, as shown below

$$|\lambda_+\rangle = |\psi_0\rangle, \quad |\lambda_-\rangle = |\psi_7\rangle \quad (40)$$

$$|\delta_+\rangle = |\psi_1\rangle, \quad |\delta_-\rangle = |\psi_6\rangle \quad (41)$$

$$|\mu_+\rangle = |\psi_2\rangle, \quad |\mu_-\rangle = |\psi_5\rangle \quad (42)$$

$$|\gamma_+\rangle = |\psi_3\rangle, \quad |\gamma_-\rangle = |\psi_4\rangle. \quad (43)$$

Additionally, the realization of the QFT relies on the adiabatic following of each of the instantaneous eigenvectors

$$|\downarrow\downarrow\downarrow\rangle \longrightarrow e^{i\alpha_1} |\psi_0\rangle \quad (44)$$

$$|\downarrow\downarrow\uparrow\rangle \longrightarrow e^{i(\alpha_2 - \frac{\pi}{2})} |\psi_1\rangle \quad (45)$$

$$|\downarrow\uparrow\downarrow\rangle \longrightarrow e^{i\alpha_3} |\psi_2\rangle \quad (46)$$

$$|\downarrow\uparrow\uparrow\rangle \longrightarrow e^{i\alpha_4} |\psi_3\rangle \quad (47)$$

$$|\uparrow\downarrow\downarrow\rangle \longrightarrow e^{-i\alpha_4} |\psi_4\rangle \quad (48)$$

$$|\uparrow\downarrow\uparrow\rangle \longrightarrow e^{-i\alpha_3} |\psi_5\rangle \quad (49)$$

$$|\uparrow\uparrow\downarrow\rangle \longrightarrow e^{-i\alpha_2} |\psi_6\rangle \quad (50)$$

$$|\uparrow\uparrow\uparrow\rangle \longrightarrow e^{-i\alpha_1} |\psi_7\rangle \quad (51)$$

and the global adiabatic phases α_j appear due to the adiabatic evolution [20, 22, 27, 28]

$$\alpha_1 = \int_{t_i}^{t_f} \lambda_+(t) dt, \quad \alpha_2 = \int_{t_i}^{t_f} \delta_+(t) dt, \quad \alpha_3 = \int_{t_i}^{t_f} \mu_+(t) dt, \quad \alpha_4 = \int_{t_i}^{t_f} \gamma_+(t) dt \quad (52)$$

with the relations

$$\lambda_-(t) = -\lambda_+(t), \quad \delta_-(t) = -\delta_+(t), \quad \mu_-(t) = -\mu_+(t), \quad \gamma_-(t) = -\gamma_+(t). \quad (53)$$

After a specific tuning of the detuning $\Delta_j(t)$, α_j reduce to

$$\alpha_1 = 2p\pi, \quad \alpha_2 = 2m\pi, \quad \alpha_3 = 2n\pi, \quad \alpha_4 = 2k\pi \quad (54)$$

with p, m, n, k are four integer numbers. This choice leads to the realization of the following unitary quantum gate

$$\mathcal{G} = \frac{1}{2\sqrt{2}} \begin{pmatrix} 1 & -i & 1 & 1 & 1 & 1 & 1 & 1 \\ 1 & -i\omega & i & i\omega & -1 & -\omega & -i & -i\omega \\ 1 & 1 & -1 & -i & 1 & i & -1 & -i \\ 1 & \omega & -i & \omega & -1 & -i\omega & i & -\omega \\ 1 & i & 1 & -1 & 1 & -1 & 1 & -1 \\ 1 & i\omega & i & -i\omega & -1 & \omega & -i & i\omega \\ 1 & -1 & -1 & i & 1 & -i & -1 & i \\ 1 & -\omega & -i & -\omega & -1 & i\omega & i & \omega \end{pmatrix}. \quad (55)$$

As a result, one can show that up to an additional phase $-\frac{\pi}{2}$ the determinant of \mathcal{G} is equal to one, i.e. $\det(\mathcal{G}) = 1$, which is necessary for adiabatic evolution. Therefore, it is worthwhile to note that the gate \mathcal{G} is a QFT one.

3.2 Controlling by Rabi frequencies

Now we will discuss how to control the Rabi frequencies $\Omega_2(t)$ and $\Omega_3(t)$ by considering the Hamiltonian $H^{(1)}(t)$ (B.2) in Appendix B without using the energy offset $H_0(t)$ (22). To achieve this goal, we drive $\Omega_2(t)$ and $\Omega_3(t)$ in a way that they become equal to the couplings J_1 and J , respectively. In what follows, we summarize the process of control in three steps.

- **Initially:** Let us assume that $\Omega_2(t_i) \gg J_1$ and $\Omega_3(t_i) \gg J$, then the eigenvectors of $H^{(1)}(t)$ (B.2) are the rotating computational spin states $|\psi(t_i)\rangle = |s'_1 s'_2 s'_3\rangle$ ($s'_j = \pm_j$), such as

$$\begin{aligned} |\pm_1\rangle &= \frac{1}{\sqrt{2}} (|\downarrow_1\rangle \pm |\uparrow_1\rangle) \\ |\pm_2\rangle &= \frac{1}{\sqrt{2}} (e^{i\varphi} |\downarrow_2\rangle \pm |\uparrow_2\rangle) \\ |\pm_3\rangle &= \frac{1}{\sqrt{2}} (|\downarrow_3\rangle \pm |\uparrow_3\rangle). \end{aligned} \quad (56)$$

- **Transition:** The adiabatic transition from the initial eigenvectors to Fourier modes is given by the mappings

$$\begin{aligned} |---\rangle &\longrightarrow e^{-i\beta_0} |\psi_0\rangle \\ |--+\rangle &\longrightarrow e^{-i\beta_1} |\psi_1\rangle \\ |-+-\rangle &\longrightarrow e^{-i\beta_2} |\psi_2\rangle \\ |-++\rangle &\longrightarrow e^{-i\beta_3} |\psi_3\rangle \\ +- --\rangle &\longrightarrow e^{-i\beta_4} |\psi_4\rangle \\ +- +-\rangle &\longrightarrow e^{-i\beta_5} |\psi_5\rangle \\ +++-\rangle &\longrightarrow e^{-i\beta_6} |\psi_6\rangle \\ ++++\rangle &\longrightarrow e^{-i\beta_7} |\psi_7\rangle \end{aligned} \quad (57)$$

where the adiabatic phases β_i read as

$$\beta_i = \int_{t_i}^{t_f} \Lambda_i(t) dt, \quad i = 1, \dots, 7 \quad (58)$$

and [Appendix B](#) shows the eigenfrequencies $\Lambda_i(t)$ ([B.3-B.10](#)) of $H^{(1)}(t)$ ([B.2](#)).

- **Finally:** We adiabatically decrease $\Omega_2(t)$ together with $\Omega_3(t)$ to end up with

$$\Omega_2(t_f) = J_1, \quad \Omega_3(t_f) = J. \quad (59)$$

As a result, the circulant symmetry will be established, and the Fourier modes will be derived as well.

At this stage, we mention that in the case of the gate realization based on the energy offset, the exact eigenvectors of the Hamiltonian ([23](#)) can not be obtained exactly. However, under the consideration made here, the derivation of eigenvectors can be achieved, see [Appendix B](#). Thus, to accelerate the gate, we combine the gate scheme with the short-cut to adiabaticity.

4 Gate implementation

To give a physical implementation of our system, we generalize the process proposed by Ivanov and Vitanov [[20](#)] to the three qubit case with trilinear coupling. Indeed, to realize the circulant Hamiltonian, we proceed with trapped ions [[29-31](#)]. A crystal with $3N$ ions with mass M is considered, the trap axis are z and x with the frequencies Ω_z and Ω_x , respectively. Each ion of the crystal is a qubit described by two typical levels: $|\uparrow\rangle, |\downarrow\rangle$ with an energy gap ω_0 . Moreover, the virtual excitations generated between two coupled ions undergo small radial vibrations around the equilibrium positions of the ions. Then, as an illustration, we present our physical implementation, depicted in [Figure 2](#).

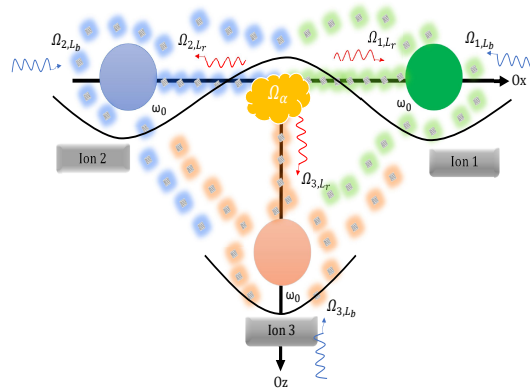


Figure 2 – (color online) A proposal for the physical implementation of the interaction between three coupled trapped ions with laser frequencies $\Omega_{j,L_r} = \omega_0 - \nu - \Delta_j(t)$ and $\Omega_{j,L_b} = \omega_0 + \nu - \Delta_j(t)$ that generates a spin-dependent force at the frequency ν .

As for our Hamiltonian ([1](#)), the implementation of kinetic terms together with bilinear couplings is perfectly discussed in [[20](#)]. Regarding the implementation of the trilinear coupling, we suggest that

it can be seen as a coupling between two coupled ions with an extra third ion [25]. To be clear, the small radial vibrations around the equilibrium positions between two coupled ions are displayed by a set of collective vibrational modes with the Hamiltonians [23, 32]

$$H_{\text{ph1}} = \sum_n \Omega_n \hat{a}_n^\dagger \hat{a}_n, \quad H_{\text{ph2}} = \sum_n \Omega_n \hat{b}_n^\dagger \hat{b}_n, \quad H_{\text{ph3}} = \sum_n \Omega_n \hat{c}_n^\dagger \hat{c}_n \quad (60)$$

whereas the internal energy is

$$H_{\text{q}} = \frac{1}{2} \sum_j \omega_0 \sigma_j^z. \quad (61)$$

and the free Hamiltonian then becomes

$$H_0 = H_{\text{q}} + \sum_j H_{\text{phj}}. \quad (62)$$

As claimed above, generating the trilinear coupling will be dependent on the interaction between two coupled ions and a third one. For instance, this can be achieved by using two pairs of noncopropagating laser beams along the radial directions of frequencies

$$\Omega_{j,L_r} = \omega_0 - \nu - \Delta_j(t) \quad (63)$$

$$\Omega_{j,L_b} = \omega_0 + \nu - \Delta_j(t) \quad (64)$$

that generate a spin-dependent force at frequency ν .

Besides, using the weak coupling assumption, one can legitimately apply the optical rotating-wave approximation and, as a result, the interacting part of our system reads now as

$$\begin{aligned} H_1 = & \sum_j \Delta_j \sigma_j^z + \Omega_x e^{ik\hat{x}_1} \cos(\nu t) \left(\sigma_1^+ e^{i\phi_1} + \sigma_1^- e^{-i\phi_1} \right) + \Omega_x e^{ik\hat{x}_2} \cos(\nu t) \left(\sigma_2^+ e^{i\phi_2} + \sigma_2^- e^{-i\phi_2} \right) \\ & + \Omega_z e^{ik\hat{z}_3} \cos(\nu t) \left(\sigma_3^+ e^{i\phi_3} + \sigma_3^- e^{-i\phi_3} \right) + \sum_j \Omega_j \left(\sigma_j^+ e^{i\theta_j} + \sigma_j^- e^{-i\theta_j} \right) \\ & + \Omega_\alpha e^{ik\hat{z}_3} \sin(\nu t) \left(\sigma_1^+ e^{i\varphi_1} + \sigma_1^- e^{-i\varphi_1} \right) \left(\sigma_2^+ e^{i\varphi_2} + \sigma_2^- e^{-i\varphi_2} \right) \end{aligned} \quad (65)$$

where $\Omega_x, \Omega_z, \Omega_j, \Omega_\alpha$ are the Rabi frequencies, ϕ_j, θ_j are the laser phases, $\varphi_{1,2}$ are the phases resulted from trilinear interaction, and the spatial arguments

$$k\hat{x}_1 = \sum_n \eta_{1,n} (\hat{a}_n^\dagger e^{i\Omega_n t} + \hat{a}_n e^{-i\Omega_n t}) \quad (66)$$

$$k\hat{x}_2 = \sum_n \eta_{2,n} (\hat{b}_n^\dagger e^{i\Omega_n t} + \hat{b}_n e^{-i\Omega_n t}) \quad (67)$$

$$k\hat{z}_3 = \sum_n \eta_{3,n} (\hat{c}_n^\dagger e^{i\Omega_n t} + \hat{c}_n e^{-i\Omega_n t}) \quad (68)$$

are involving the Lamb-Dicke parameters

$$\eta_{j,n} = b_{j,n} k \sqrt{\hbar/2M\Omega_n} \quad (69)$$

with $b_{j,n}$ are the normal mode transformation matrix for the j^{th} ion. Hence, since the dimensionless parameter $\eta_{j,n}$ is small, we can make the Lamb-Dicke approximation, $\Delta k \langle \hat{x}_1 \rangle \ll 1$, $\Delta k \langle \hat{x}_2 \rangle \ll 1$,

$\Delta k \langle \hat{z}_3 \rangle \ll 1$, to end up with

$$\begin{aligned}
H_1 = & \sum_j \Delta_j \sigma_j^z + \sum_n J_{1,n} \cos(\nu t) \left(\sigma_1^+ e^{i\phi_1} + \sigma_1^- e^{-i\phi_1} \right) \left(\hat{a}_n^\dagger e^{i\Omega_n t} + \hat{a}_n e^{-i\Omega_n t} \right) \\
& + \sum_j \Omega_j \left(\sigma_j^+ e^{i\theta_j} + \sigma_j^- e^{-i\theta_j} \right) + \sum_n J_{2,n} \cos(\nu t) \left(\sigma_2^+ e^{i\phi_2} + \sigma_2^- e^{-i\phi_2} \right) \left(\hat{b}_n^\dagger e^{i\Omega_n t} + \hat{b}_n e^{-i\Omega_n t} \right) \\
& + \sum_n J_{3,n} \cos(\nu t) \left(\sigma_3^+ e^{i\phi_3} + \sigma_3^- e^{-i\phi_3} \right) \left(\hat{c}_n^\dagger e^{i\Omega_n t} + \hat{c}_n e^{-i\Omega_n t} \right) \\
& + \sum_n h_n \sin(\nu t) \left(\sigma_1^+ e^{i\varphi_1} + \sigma_1^- e^{-i\varphi_1} \right) \left(\sigma_2^+ e^{i\varphi_2} + \sigma_2^- e^{-i\varphi_2} \right) \left(\hat{c}_n^\dagger e^{i\Omega_n t} + \hat{c}_n e^{-i\Omega_n t} \right)
\end{aligned} \tag{70}$$

where $J_{1,n} = \eta_{1,n} \Omega_x$, $J_{2,n} = \eta_{2,n} \Omega_x$ and $J_{3,n} = \eta_{3,n} \Omega_z$ are the spin-phonon coupling and $h_n = \eta_{3,n} \Omega_\alpha$ is the trilinear coupling. Moreover, during a slow dynamics, the beat-note frequency ν isn't resonant with any radial vibration mode, i.e. $|\Omega_n - \nu| \gg J_{j,n}, h_n$. Additionally, if the phonons are virtually excited, then they should be eliminated from the dynamics, and as a consequence, the spin states in different sites become coupled to each other. For the different three sites j^{th} , p^{th} and q^{th} , we have

$$\begin{aligned}
H_1 = & \Delta_j \sigma_j^z + \Delta_p \sigma_p^z + \Delta_q \sigma_q^z + \Omega_j \left(\sigma_j^+ e^{i\theta_j} + \sigma_j^- e^{-i\theta_j} \right) + \Omega_p \left(\sigma_p^+ e^{i\theta_p} + \sigma_p^- e^{-i\theta_p} \right) \\
& + \Omega_q \left(\sigma_q^+ e^{i\theta_q} + \sigma_q^- e^{-i\theta_q} \right) + J_1 \left(\sigma_j^+ e^{i\phi_j} + \sigma_j^- e^{-i\phi_j} \right) \left(\sigma_p^+ e^{i\phi_p} + \sigma_p^- e^{-i\phi_p} \right) \\
& + J_2 \left(\sigma_p^+ e^{i\phi_p} + \sigma_p^- e^{-i\phi_p} \right) \left(\sigma_q^+ e^{i\phi_q} + \sigma_q^- e^{-i\phi_q} \right) + J_3 \left(\sigma_j^+ e^{i\phi_j} + \sigma_j^- e^{-i\phi_j} \right) \left(\sigma_q^+ e^{i\phi_q} + \sigma_q^- e^{-i\phi_q} \right) \\
& + J \left(\sigma_j^+ e^{i\varphi_j} + \sigma_j^- e^{-i\varphi_j} \right) \left(\sigma_p^+ e^{i\varphi_p} + \sigma_p^- e^{-i\varphi_p} \right) \left(\sigma_q^+ e^{i\varphi_q} + \sigma_q^- e^{-i\varphi_q} \right)
\end{aligned} \tag{71}$$

where the couplings between two ions are given by

$$J_1 = \sum_n J_{j,n} J_{p,n} \frac{1}{\nu^2 - \Omega_n^2}, \quad J_2 = \sum_n J_{p,n} J_{q,n} \frac{1}{\nu^2 - \Omega_n^2}, \quad J_3 = \sum_n J_{j,n} J_{q,n} \frac{1}{\nu^2 - \Omega_n^2} \tag{72}$$

and that of the trilinear coupling between three ions

$$J = \sum_n J_{j,n} J_{p,n} h_n \frac{1}{\nu^2 - \Omega_n^2}. \tag{73}$$

At this level, it is clearly seen that one can realize the circulant Hamiltonian $H_{\text{cir}}^{(1)}(t)$ (16) by adjusting the coupling parameters.

5 Numerical analysis

In what follows, we choose the following time modulations of the couplings $J_1(t)$, $J(t)$ and the detunings $\Delta_j(t)$ for the gate implementation:

$$J_1(t) = J_{01} \sin^2(\omega' t) \tag{74}$$

$$J(t) = J_0 \sin^2(\omega' t) \tag{75}$$

$$\Delta_j(t) = \Delta_j \cos^2(\omega' t) \tag{76}$$

where the characteristic parameter ω' controls the adiabaticity of the transition and the interaction time t varies as $t \in [0, t_{max}]$ with $t_{max} = \frac{\pi}{2\omega'}$. This time dependence guarantees the following conditions

$$\Delta_{1,2,3}(0) \gg J(0), J_1(0), \quad \Delta_{1,2,3}(t_{max}) \ll J(t_{max}), J_1(t_{max}). \tag{77}$$

The adiabatic transition to Fourier modes can be carried out without using the detuning Δ_j . In fact, we can simply vary the Rabi frequencies to finally get the Fourier modes, such as

$$J(t) = J_0 \sin^2(\omega't) \quad (78)$$

$$J_1(t) = J_{01} \sin^2(\omega't) \quad (79)$$

$$\Omega_2(t) = J_{01} + \Upsilon_0 \cos^2(\omega't) \quad (80)$$

$$\Omega_3(t) = J_0 + \Upsilon'_0 \cos^2(\omega't) \quad (81)$$

with Υ_0 and Υ'_0 are the adding amplitudes for the control of the adiabaticity of transition in the second and third qubits, respectively.

5.1 Eigenfrequencies

We numerically show in **Figure 3** the eigenfrequencies $\lambda_{\pm}(t), \delta_{\pm}(t), \mu_{\pm}(t), \gamma_{\pm}(t)$ of the Hamiltonian $H(t)$ (23) versus time under suitable choices of the coupling parameters and detunings. As expected, all eigenfrequencies are separated from each other, which entails, in its turn the suppression of any transition to a superposition of eigenstates. The degeneracy of the energies should be avoided during the simulated time, and this is due to the fact that degeneracy entails the prevention of the gate implementation at hand. The gap between the eigenvalues decreases during the simulation time. To avoid their degeneracy during the evolution, we have introduced the detuning frequencies Δ_j . Additionally, we mention that the amplitude couplings J_0 and J_{01} are important to prevent the degeneracy at final time t_{max} .

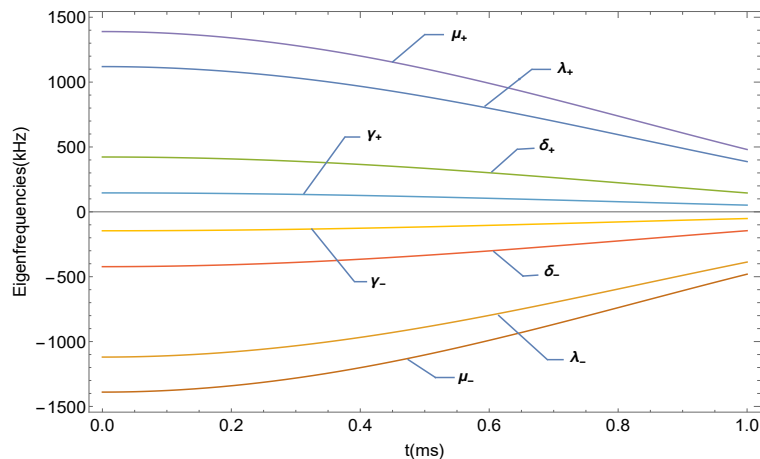


Figure 3 – (color online) Eigenfrequencies of the Hamiltonian $H(t)$ (23) as a function of the time. The parameters are chosen as $J_0/2\pi = 1$ kHz, $J_{01}/2\pi = 2$ kHz, $\Delta_1/2\pi = 120$ kHz, $\Delta_2/2\pi = 60$ kHz, $\Delta_3/2\pi = 30$ kHz, $\varphi = \frac{\pi}{2}$, $\omega'/2\pi = 0.15$ kHz.

5.2 Gate fidelity

Gate fidelity is a tool to compare how close two gates, or more generally operations, are to each other [33]. In other words, it expresses the probability that one state will pass a test to identify itself as the other one. We recall that fidelities higher than 99.99% for a single-qubit gate and 99.9 % for

an entangling gate in a two-ion crystal have been developed in [34–36]. Generally, for the theoretical density matrix ρ_0 and reconstructed density matrix ρ , it is defined by

$$F(\rho_0, \rho) = \left(\text{Tr} \sqrt{\sqrt{\rho_0} \rho \sqrt{\rho_0}} \right)^2. \quad (82)$$

By applying the Uhlmann theorem [37], (82) can take a simple form

$$F(\rho_0, \rho) = |\langle \psi_0 | \psi \rangle|^2. \quad (83)$$

with ψ_0 and ψ are theoretical and reconstructed purified state vectors, respectively. As for our system, we have [20]

$$F_{\text{Gate}}(t) = \frac{1}{16} \left| \sum_{s_1, s_2, s_3} \langle s_1 s_2 s_3 | \mathcal{G}^\dagger \mathcal{G}'(t) | s_1 s_2 s_3 \rangle \right|^2 \quad (84)$$

where $s_j = \uparrow_j, \downarrow_j$, \mathcal{G} is the three-qubit QFT (55) and $\mathcal{G}'(t)$ is the real transform. In Figure 4, we present the gate fidelity versus the evolution time by choosing the detunings $\Delta_{1,2,3}$ such that the adiabatic phases are given in (54). The unitary propagator $\mathcal{G}'(t)$ converges to \mathcal{G} as time progresses. We notice that for a nonlinear coupling $J_0 = 1$ kHz and $t = 0.4875$ ms, the gate reaches a high fidelity (96%).

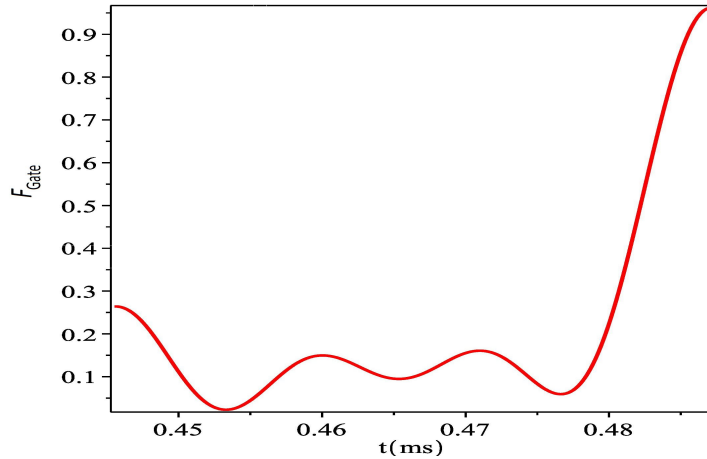


Figure 4 – (color online) The gate fidelity is calculated using the Hamiltonian $H(t)$ (23) in a numerical simulation. The parameters are chosen as $J_0/2\pi = J_{01}/2\pi = 1$ kHz, $\Delta_1/2\pi = 20$ kHz, $\Delta_2/2\pi = 10$ kHz, $\Delta_3/2\pi = 6$ kHz, $\varphi = \frac{\pi}{2}$ and $\omega' = 0.505$ kHz.

By using the Hamiltonian (B.2) together with the quantum Fourier states (3-10), one can end up with the fidelity of the adiabatic transitions between the rotating computational spin states $|s'_1 s'_2 s'_3\rangle$ ($s'_j = \pm_j$)

$$F_{\text{ad}}(t) = \frac{1}{16} \left| \sum_{i=0}^{i=7} \langle \psi_i | \Lambda_i \rangle \right|^2 \quad (85)$$

and more explicitly, we have

$$F_{\text{ad}}(t) = \frac{1}{16} |\langle \psi_0 | \Lambda_0 \rangle + \langle \psi_1 | \Lambda_1 \rangle + \langle \psi_2 | \Lambda_2 \rangle + \langle \psi_3 | \Lambda_3 \rangle + \langle \psi_4 | \Lambda_4 \rangle + \langle \psi_5 | \Lambda_5 \rangle + \langle \psi_6 | \Lambda_6 \rangle + \langle \psi_7 | \Lambda_7 \rangle|^2. \quad (86)$$

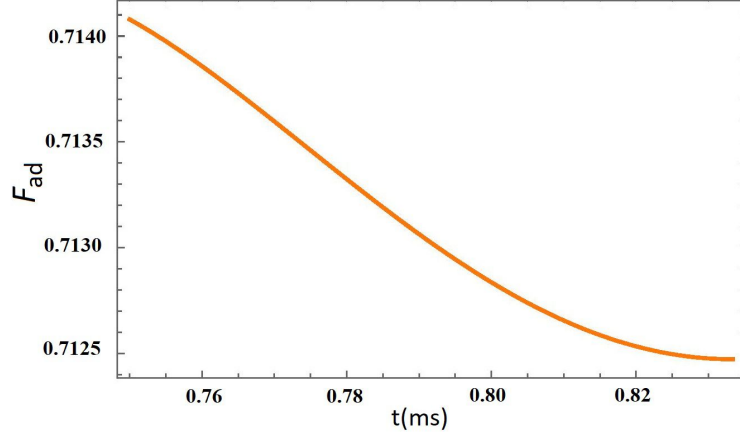


Figure 5 – (color online) Fidelity of adiabatic transition with $J_0/2\pi = 2.1$ kHz, $\Upsilon_0/2\pi = 1.9$ kHz, $J_{01}/2\pi = 2.4$ kHz, $\Upsilon'_0/2\pi = 2$ kHz, $\varphi = \frac{\pi}{4}$ and $\omega'/2\pi = 0.3$ kHz.

Figure 5 presents the good fidelity of the adiabatic transition within a shorter interaction time, $t_{max} = 0.835$ ms. It is clearly seen that our results show the possibility for obtaining high fidelity (71%).

5.3 Creation of entangled states

To create entangled states, one has to suitably prepare the initial state in a superposition of spin states, which is due to the fact that the action of the QFT on the computational basis creates a superposition, but they are not entangled. For concreteness, we assume that the system is initially prepared in the following state:

$$|\psi(0)\rangle = \frac{1}{2} |\downarrow_1\rangle (e^{i\alpha_1} |\downarrow_2\downarrow_3\rangle + e^{i\alpha_2} |\downarrow_2\uparrow_3\rangle + e^{i\alpha_3} |\uparrow_2\downarrow_3\rangle + e^{i\alpha_4} |\uparrow_2\uparrow_3\rangle). \quad (87)$$

Performing our three qubit gates, we obtain the entangled state

$$|\psi(0)\rangle \longrightarrow |\psi(t_f)\rangle = \frac{1}{2} (|\psi_0\rangle + |\psi_1\rangle + |\psi_2\rangle + |\psi_3\rangle). \quad (88)$$

Let us emphasize that by rotating the initially prepared state such as

$$|\psi(0)\rangle = \frac{1}{2} |-1\rangle (e^{-i\beta_0} |-2-3\rangle + e^{-i\beta_1} |-2+3\rangle + e^{-i\beta_2} |+2-3\rangle + e^{-i\beta_3} |+2+3\rangle) \quad (89)$$

we end up with the same transformed entangled state (88). Therefore, the fidelity of the creation of the entangled state is defined by

$$F(t) = \frac{1}{2} |\langle \psi(t_f) | (e^{-i\beta_0} |\Lambda_0(t)\rangle + e^{-i\beta_1} |\Lambda_1(t)\rangle + e^{-i\beta_2} |\Lambda_2(t)\rangle + e^{-i\beta_3} |\Lambda_3(t)\rangle) \rangle|^2. \quad (90)$$

By adjusting the parameters ω' , J_{01} and J_0 one can achieve high fidelity in the creation of entangled states as presented in **Figure 6-A**, **Figure 6-B** and **Figure 6-C**.

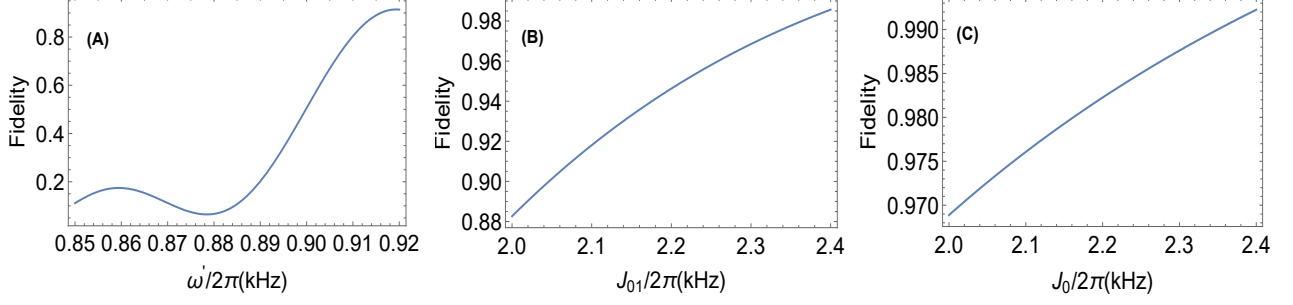


Figure 6 – (color online) The fidelity of the entangled state is calculated from the numerical simulation of the Hamiltonian (B.2). (A): $\Upsilon_0 = 1.8$ kHz, $\Upsilon'_0 = 1.7$ kHz, $J_{01} = 2.1$ kHz, $J_0 = 2.3$ kHz and the gate time $t = 0.31$ ms. (B): The same values with $\omega'/2\pi = 0.5$ kHz and vary the coupling strength J_{01} . (C): The same values in (A) with $\omega'/2\pi = 0.605$ kHz and vary the coupling strength J_0 .

6 Short-cut to adiabaticity

Now we add an auxiliary interaction $H_{\text{CD}}(t)$ (counter-driving-field) [22,38] to the reference Hamiltonian $H^{(1)}(t)$ (B.2) in order to suppress the non-adiabatic transitions and reduce the gate time. As a result, the Hamiltonian will take the following form:

$$H_{\text{T}}(t) = H^{(1)}(t) + H_{\text{CD}}(t) \quad (91)$$

such that the interaction is

$$H_{\text{CD}}(t) = i\hbar \sum_{i=0}^7 |\partial_t \Lambda_i(t)\rangle \langle \Lambda_i(t)| \quad (92)$$

and (B.11-B.18) show the time-dependent eigenvectors $|\Lambda_i(t)\rangle$ of $H^{(1)}(t)$. After some algebra, we obtain

$$H_{\text{CD}}(t) = -\partial_t \kappa(t) \begin{pmatrix} 0 & 0 & 0 & 0 & 1 & 0 & 0 & 0 \\ 0 & 0 & 0 & 0 & 0 & 1 & 0 & 0 \\ 0 & 0 & 0 & 0 & 0 & 0 & 0 & 0 \\ 0 & 0 & 0 & 0 & 0 & 0 & 0 & 0 \\ 1 & 0 & 0 & 0 & 0 & 0 & 0 & 0 \\ 0 & 1 & 0 & 0 & 0 & 0 & 0 & 0 \\ 0 & 0 & 0 & 0 & 0 & 0 & 0 & 0 \\ 0 & 0 & 0 & 0 & 0 & 0 & 0 & 0 \end{pmatrix}. \quad (93)$$

Using the time-dependent coupling parameters (78-81) and the eigenvectors (B.11-B.18), we explicitly determine the counter-driving-field

$$\partial_t \kappa(t) = \frac{1}{2} \left(\frac{\omega' J_{01} (J_{01} + \Upsilon_0) \sin(2\omega't)}{J_{01}^2 \sin^4(\omega't) + [\Upsilon_0 \sin^2(\omega't) - (J_{01} + \Upsilon_0)]^2} + \frac{\omega' J_0 (J_0 + \Upsilon'_0) \sin(2\omega't)}{J_0^2 \sin^4(\omega't) + [\Upsilon'_0 \sin^2(\omega't) - (J_0 + \Upsilon'_0)]^2} \right). \quad (94)$$

In Figure 7, we show the shape of the counter-driving field (94) as a function of the time and by varying ω' , J_{01} and J_0 . The counter-driving term should be zero at $t = 0$, because the system starts

in the rotational computational spin states. We mention also that at t_{max} , the system ends up with the Fourier modes.

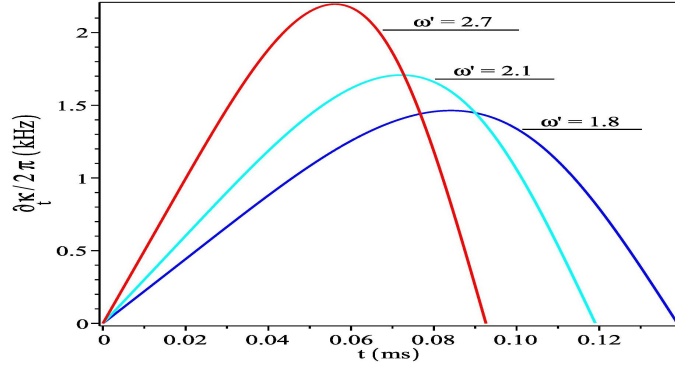


Figure 7 – (color online) Behavior of a counter-driving field with $\Upsilon_0/2\pi = 0.5$ kHz and $\Upsilon'_0/2\pi = 2$ kHz, while the remaining parameters are chosen as $J_{01} = 1.5$ kHz, $J_0 = 1$ kHz (blue line), $J_{01} = 1.9$ kHz, $J_0 = 1.3$ kHz (cyan line), $J_{01} = 2$ kHz, $J_0 = 1.7$ kHz (red line).

7 Conclusion

We generalized the work done by Ivanov and Vitanov [20] dealing with two-qubit quantum gates and entanglement protected by circulant symmetry to a system of three-qubit quantum gates. In fact, we have constructed a discrete system based on three qubits emerging in a magnetic field. A special symmetry called circulant can be obtained only by adjusting the Rabi frequencies and the coupling parameters characterizing our system. We have shown that our eigenvectors do not depend on the magnitude of the physical parameters, which entails the protection of entanglement. These eigenvectors lead to obtaining the quantum Fourier transform (QFT) modes, which imply the realization of a QFT gate. To discuss the implementation of the gate, the eigenfrequencies should be non-degenerate. For this aim, we have added an Hamiltonian $H_0(t)$ that breaks the circulant symmetry and favors the adiabatic transition process.

Subsequently, instead of adding an energy offset, we have shown that it is possible to control the transition by using only the Rabi frequencies. As a result, the gate scheme with the short-cut to adiabaticity has been discussed, and therefore we have found the suppression of the non-adiabatic transition and the acceleration of the gate. Additionally, in the framework of the trapped ions, we have suggested a possible physical implementation of the constructed Hamiltonian. By assuming a particular sinusoidal modulation, several fidelities are discussed, and the results show the possibility to achieve high fidelities only by adjusting the physical parameters. The physical realization of a three-qubit QFT is the key subroutine in several quantum algorithms. Then, it turns out that our present three-qubit gates can significantly reduce the number of gates in a quantum algorithm.

In this work, we have added the trilinear coupling, which is necessary to retain the circulant symmetry in a three-qubit system. Indeed, a three-qubit system with only bilinear interaction terms, as done in [18], does not lead to the wanted circulant symmetry. Additionally, constructing a circulant Hamiltonian based on N -qubits is not obvious. Indeed, the Hamiltonian demands multilinear interaction terms that are not easily realizable. Moreover, discussing the adiabatic transition and accelerating the gate using a shortcut to adiabaticity will be hard.

Appendix A Eigenfrequencies of $H(t)$ with energy offset

As for $H(t)$ (23) including the circulant Hamiltonian (16) and the energy offset (22), we show that the corresponding eigenfrequencies are given by

$$\lambda_{\pm} = \pm \sqrt{\left| -\frac{A}{4} - S + \frac{1}{2} \sqrt{-4S^2 - 2p + \frac{q}{S}} \right|} \quad (\text{A.1})$$

$$\delta_{\pm} = \pm \sqrt{\left| -\frac{A}{4} - S - \frac{1}{2} \sqrt{-4S^2 - 2p + \frac{q}{S}} \right|} \quad (\text{A.2})$$

$$\mu_{\pm} = \pm \sqrt{\left| -\frac{A}{4} + S + \frac{1}{2} \sqrt{-4S^2 - 2p - \frac{q}{S}} \right|} \quad (\text{A.3})$$

$$\gamma_{\pm} = \pm \sqrt{\left| -\frac{A}{4} + S - \frac{1}{2} \sqrt{-4S^2 - 2p - \frac{q}{S}} \right|} \quad (\text{A.4})$$

where we have set

$$p = \frac{1}{8}(8B - 3) \quad (\text{A.5})$$

$$q = \frac{1}{8}(-1 + 4B + 8C) \quad (\text{A.6})$$

$$S = \frac{1}{2} \sqrt{\frac{1}{3} \left| -2p + \left(Q + \frac{\Delta_0}{Q} \right) \right|} \quad (\text{A.7})$$

$$\Delta_0 = B^2 + 3C + 12D \quad (\text{A.8})$$

$$Q = \sqrt[3]{\frac{1}{2} \left| \Delta + \sqrt{|\Delta^2 - 4\Delta_0^3|} \right|} \quad (\text{A.9})$$

$$\Delta = 2B^3 + 9BC + 27D + 27C^2 - 72BD \quad (\text{A.10})$$

and the associated quantities are

$$\begin{aligned} A &= -16J^2 - 4\Delta_1^2 - 4\Delta_2^2 - 4\Delta_3^2 - 8J_1^2 \\ B &= 32J^2\Delta_1^2 + 32J^2\Delta_2^2 + 48J^2\Delta_3^2 + 128J^2J_1^2 + 6\Delta_1^4 + 4\Delta_1^2\Delta_2^2 + 4\Delta_1^2\Delta_3^2 \\ &\quad + 16\Delta_1^2J_1^2 + 6\Delta_2^4 + 4\Delta_2^2\Delta_3^2 + 24\Delta_2^2J_1^2 + 6\Delta_3^4 + 8\Delta_3^2J_1^2 + 16J_1^4 \\ C &= -16J^2\Delta_1^4 - 32J^2\Delta_1^2\Delta_2^2 - 128J^2\Delta_1^2J_1^2 - 16J^2\Delta_2^4 - 128J^2\Delta_2^2J_1^2 \\ &\quad - 48J^2\Delta_3^4 - 256J^2J_1^4 - 4\Delta_1^6 + 4\Delta_1^4\Delta_2^2 + 4\Delta_1^4\Delta_3^2 - 8\Delta_1^4J_1^2 + 4\Delta_1^2\Delta_2^4 \\ &\quad - 40\Delta_1^2\Delta_2^2\Delta_3^2 + 4\Delta_1^2\Delta_3^4 - 32\Delta_1^2\Delta_3^2J_1^2 - 4\Delta_2^6 + 4\Delta_2^4\Delta_3^2 - 24\Delta_2^4J_1^2 \\ &\quad + 4\Delta_2^2\Delta_3^4 + 16\Delta_2^2\Delta_3^2J_1^2 - 32\Delta_2^2J_1^4 - 4\Delta_3^6 + 8\Delta_3^4J_1^2 - 32\Delta_3^2J_1^4 \\ D &= 4\Delta_1^4\Delta_2^2\Delta_3^2 + 4\Delta_1^2\Delta_2^4\Delta_3^2 + 4\Delta_1^2\Delta_2^2\Delta_3^4 - 4\Delta_1^6\Delta_2^2 - 4\Delta_1^6\Delta_3^2 + 6\Delta_1^4\Delta_2^4 \\ &\quad + 6\Delta_1^4\Delta_3^4 - 4\Delta_1^2\Delta_2^6 - 4\Delta_1^2\Delta_3^6 - 4\Delta_2^6\Delta_3^2 + 6\Delta_2^4\Delta_3^4 - 4\Delta_2^2\Delta_3^6 + 16\Delta_2^4J_1^4 \\ &\quad - 8\Delta_3^6J_1^2 + 16\Delta_3^4J_1^4 + 16J^2\Delta_3^6 + 8\Delta_2^6J_1^2 + 16\Delta_1^2\Delta_3^4J_1^2 - 24\Delta_2^4\Delta_3^2J_1^2 \\ &\quad + 24\Delta_2^2\Delta_3^4J_1^2 - 32\Delta_2^2\Delta_3^2J_1^4 + 8\Delta_1^4\Delta_2^2J_1^2 - 8\Delta_1^4\Delta_3^2J_1^2 - 16\Delta_1^2\Delta_2^4J_1^2 \\ &\quad - 128J^2\Delta_3^4J_1^2 + 256J^2\Delta_3^2J_1^4 + 16J^2\Delta_1^4\Delta_3^2 - 32J^2\Delta_1^2\Delta_3^4 + 16J^2\Delta_2^4\Delta_3^2 \\ &\quad - 32J^2\Delta_2^2\Delta_3^4 + 32J^2\Delta_1^2\Delta_2^2\Delta_3^2 + 128J^2\Delta_1^2\Delta_3^2J_1^2 + 128J^2\Delta_2^2\Delta_3^2J_1^2 + \Delta_1^8 + \Delta_2^8 + \Delta_3^8. \end{aligned}$$

Appendix B Energy spectrum of $H^{(1)}(t)$

The Hamiltonian $H^{(1)}(t)$ with $\Omega_2(t)$ (i.e. $J_1 = \Omega_2(t)$ and $J = \Omega_3(t)$ are not always respected) has the following form:

$$\begin{aligned}
H^{(1)}(t) = & J_1(\sigma_1^+ + \sigma_1^-)(\sigma_2^+ e^{-i\varphi} + \sigma_2^- e^{i\varphi}) + \Omega_3(t)(\sigma_2^+ + \sigma_2^-)(\sigma_3^+ e^{-i\varphi} + \sigma_3^- e^{i\varphi}) \\
& + \Omega_3(t)(\sigma_1^+ + \sigma_1^-)(\sigma_3^+ e^{i\varphi} + \sigma_3^- e^{-i\varphi}) + \Omega_2(t)(\sigma_2^+ e^{i\varphi} + \sigma_2^- e^{-i\varphi}) \\
& + \Omega_3(t)(\sigma_3^+ e^{i\varphi} + \sigma_3^- e^{-i\varphi}) + J(\sigma_1^+ + \sigma_1^-)(\sigma_2^+ + \sigma_2^-)(\sigma_3^+ e^{-i\varphi} + \sigma_3^- e^{i\varphi})
\end{aligned} \tag{B.1}$$

and we have in the matrix notation

$$H^{(1)}(t) = \begin{pmatrix} 0 & \Omega_3(t)e^{i\varphi} & \Omega_2(t)e^{i\varphi} & \Omega_3(t)e^{-i\varphi} & 0 & \Omega_3(t)e^{i\varphi} & J_1e^{-i\varphi} & Je^{-i\varphi} \\ \Omega_3(t)e^{-i\varphi} & 0 & \Omega_3(t)e^{i\varphi} & \Omega_2(t)e^{i\varphi} & \Omega_3(t)e^{-i\varphi} & 0 & Je^{i\varphi} & J_1e^{-i\varphi} \\ \Omega_2(t)e^{-i\varphi} & \Omega_3(t)e^{-i\varphi} & 0 & \Omega_3(t)e^{i\varphi} & J_1e^{i\varphi} & Je^{-i\varphi} & 0 & \Omega_3(t)e^{i\varphi} \\ \Omega_3(t)e^{i\varphi} & \Omega_2(t)e^{-i\varphi} & \Omega_3(t)e^{-i\varphi} & 0 & Je^{i\varphi} & J_1e^{i\varphi} & \Omega_3(t)e^{-i\varphi} & 0 \\ 0 & \Omega_3(t)e^{i\varphi} & J_1e^{-i\varphi} & Je^{-i\varphi} & 0 & \Omega_3(t)e^{i\varphi} & \Omega_2(t)e^{i\varphi} & \Omega_3(t)e^{-i\varphi} \\ \Omega_3(t)e^{-i\varphi} & 0 & Je^{i\varphi} & J_1e^{-i\varphi} & Je^{-i\varphi} & 0 & \Omega_3(t)e^{i\varphi} & \Omega_2(t)e^{i\varphi} \\ J_1e^{i\varphi} & Je^{-i\varphi} & 0 & \Omega_3(t)e^{i\varphi} & \Omega_2(t)e^{-i\varphi} & \Omega_3(t)e^{-i\varphi} & 0 & \Omega_3(t)e^{i\varphi} \\ Je^{i\varphi} & J_1e^{i\varphi} & \Omega_3(t)e^{-i\varphi} & 0 & \Omega_3(t)e^{i\varphi} & \Omega_2(t)e^{-i\varphi} & \Omega_3(t)e^{-i\varphi} & 0 \end{pmatrix}. \tag{B.2}$$

We choose $\varphi = \frac{\pi}{4}$ for simplicity and show that the time-dependent eigenfrequencies $H^{(1)}(t)$ (B.2) are given by

$$\Lambda_0(t) = \sqrt{(\Omega_3 - J)^2 + J_1^2 + \Omega_2^2 + \sqrt{2(\Omega_3 - J)^2(J_1 - \Omega_2)^2}} \tag{B.3}$$

$$\Lambda_1(t) = -\sqrt{(\Omega_3 - J)^2 + J_1^2 + \Omega_2^2 + \sqrt{2(\Omega_3 - J)^2(J_1 - \Omega_2)^2}} \tag{B.4}$$

$$\Lambda_2(t) = \sqrt{(\Omega_3 - J)^2 + J_1^2 + \Omega_2^2 - \sqrt{2(\Omega_3 - J)^2(J_1 - \Omega_2)^2}} \tag{B.5}$$

$$\Lambda_3(t) = -\sqrt{(\Omega_3 - J)^2 + J_1^2 + \Omega_2^2 - \sqrt{2(\Omega_3 - J)^2(J_1 - \Omega_2)^2}} \tag{B.6}$$

$$\Lambda_4(t) = \sqrt{5\Omega_3^2 + 2J\Omega_3 + J^2 + J_1^2 + \Omega_2^2 + \sqrt{2\Omega_3^2(9\Omega_2^2 + 2J_1\Omega_2 + 9J_1^2) + 2J(J_1 + \Omega_2)^2(2\Omega_3 + J)}} \tag{B.7}$$

$$\Lambda_5(t) = -\sqrt{5\Omega_3^2 + 2J\Omega_3 + J^2 + J_1^2 + \Omega_2^2 + \sqrt{2\Omega_3^2(9\Omega_2^2 + 2J_1\Omega_2 + 9J_1^2) + 2J(J_1 + \Omega_2)^2(2\Omega_3 + J)}} \tag{B.8}$$

$$\Lambda_6(t) = \sqrt{5\Omega_3^2 + 2J\Omega_3 + J^2 + J_1^2 + \Omega_2^2 - \sqrt{2\Omega_3^2(9\Omega_2^2 + 2J_1\Omega_2 + 9J_1^2) + 2J(J_1 + \Omega_2)^2(2\Omega_3 + J)}} \tag{B.9}$$

$$\Lambda_7(t) = -\sqrt{5\Omega_3^2 + 2J\Omega_3 + J^2 + J_1^2 + \Omega_2^2 - \sqrt{2\Omega_3^2(9\Omega_2^2 + 2J_1\Omega_2 + 9J_1^2) + 2J(J_1 + \Omega_2)^2(2\Omega_3 + J)}} \tag{B.10}$$

and the corresponding eigenvectors can be expressed as

$$|\Lambda_0(t)\rangle = \frac{1}{2\sqrt{2}} \quad (\text{B.11})$$

$$\left(e^{-i\alpha(t)} |\downarrow\downarrow\downarrow\rangle + e^{-i\alpha(t)} |\downarrow\downarrow\uparrow\rangle + |\downarrow\uparrow\downarrow\rangle + |\downarrow\uparrow\uparrow\rangle + e^{-i\alpha(t)} |\uparrow\downarrow\downarrow\rangle + e^{-i\alpha(t)} |\uparrow\downarrow\uparrow\rangle + |\uparrow\uparrow\downarrow\rangle + |\uparrow\uparrow\uparrow\rangle \right)$$

$$|\Lambda_1(t)\rangle = \frac{1}{2\sqrt{2}} \quad (\text{B.12})$$

$$\left(e^{i\alpha(t)} |\downarrow\downarrow\downarrow\rangle + \omega e^{i\alpha(t)} |\downarrow\downarrow\uparrow\rangle + i |\downarrow\uparrow\downarrow\rangle + i\omega |\downarrow\uparrow\uparrow\rangle - e^{i\alpha(t)} |\uparrow\downarrow\downarrow\rangle - \omega e^{i\alpha(t)} |\uparrow\downarrow\uparrow\rangle - i |\uparrow\uparrow\downarrow\rangle - i\omega |\uparrow\uparrow\uparrow\rangle \right)$$

$$|\Lambda_2(t)\rangle = \frac{1}{2\sqrt{2}} \quad (\text{B.13})$$

$$\left(e^{-i\alpha(t)} |\downarrow\downarrow\downarrow\rangle + i e^{-i\alpha(t)} |\downarrow\downarrow\uparrow\rangle - |\downarrow\uparrow\downarrow\rangle - i |\downarrow\uparrow\uparrow\rangle + e^{-i\alpha(t)} |\uparrow\downarrow\downarrow\rangle + i e^{-i\alpha(t)} |\uparrow\downarrow\uparrow\rangle - |\uparrow\uparrow\downarrow\rangle - i |\uparrow\uparrow\uparrow\rangle \right)$$

$$|\Lambda_3(t)\rangle = \frac{1}{2\sqrt{2}} \quad (\text{B.14})$$

$$\left(e^{i\alpha(t)} |\downarrow\downarrow\downarrow\rangle + i\omega e^{i\alpha(t)} |\downarrow\downarrow\uparrow\rangle - i |\downarrow\uparrow\downarrow\rangle + \omega |\downarrow\uparrow\uparrow\rangle - e^{i\alpha(t)} |\uparrow\downarrow\downarrow\rangle - i\omega e^{i\alpha(t)} |\uparrow\downarrow\uparrow\rangle + i |\uparrow\uparrow\downarrow\rangle - \omega |\uparrow\uparrow\uparrow\rangle \right)$$

$$|\Lambda_4(t)\rangle = \frac{1}{2\sqrt{2}} \quad (\text{B.15})$$

$$\left(e^{-i\alpha(t)} |\downarrow\downarrow\downarrow\rangle - e^{-i\alpha(t)} |\downarrow\downarrow\uparrow\rangle + |\downarrow\uparrow\downarrow\rangle - |\downarrow\uparrow\uparrow\rangle + e^{-i\alpha(t)} |\uparrow\downarrow\downarrow\rangle - e^{-i\alpha(t)} |\uparrow\downarrow\uparrow\rangle + |\uparrow\uparrow\downarrow\rangle - |\uparrow\uparrow\uparrow\rangle \right)$$

$$|\Lambda_5(t)\rangle = \frac{1}{2\sqrt{2}} \quad (\text{B.16})$$

$$\left(e^{i\alpha(t)} |\downarrow\downarrow\downarrow\rangle - \omega e^{i\alpha(t)} |\downarrow\downarrow\uparrow\rangle + i |\downarrow\uparrow\downarrow\rangle - i\omega |\downarrow\uparrow\uparrow\rangle - e^{i\alpha(t)} |\uparrow\downarrow\downarrow\rangle + \omega e^{i\alpha(t)} |\uparrow\downarrow\uparrow\rangle - i |\uparrow\uparrow\downarrow\rangle + i\omega |\uparrow\uparrow\uparrow\rangle \right)$$

$$|\Lambda_6(t)\rangle = \frac{1}{2\sqrt{2}} \quad (\text{B.17})$$

$$\left(e^{-i\alpha(t)} |\downarrow\downarrow\downarrow\rangle - i e^{-i\alpha(t)} |\downarrow\downarrow\uparrow\rangle - |\downarrow\uparrow\downarrow\rangle + i |\downarrow\uparrow\uparrow\rangle + e^{-i\alpha(t)} |\uparrow\downarrow\downarrow\rangle - i e^{-i\alpha(t)} |\uparrow\downarrow\uparrow\rangle - |\uparrow\uparrow\downarrow\rangle + i |\uparrow\uparrow\uparrow\rangle \right)$$

$$|\Lambda_7(t)\rangle = \frac{1}{2\sqrt{2}} \quad (\text{B.18})$$

$$\left(e^{i\alpha(t)} |\downarrow\downarrow\downarrow\rangle - i\omega e^{i\alpha(t)} |\downarrow\downarrow\uparrow\rangle - i |\downarrow\uparrow\downarrow\rangle - \omega |\downarrow\uparrow\uparrow\rangle - e^{i\alpha(t)} |\uparrow\downarrow\downarrow\rangle + i\omega e^{i\alpha(t)} |\uparrow\downarrow\uparrow\rangle + i |\uparrow\uparrow\downarrow\rangle + \omega |\uparrow\uparrow\uparrow\rangle \right)$$

where we have defined

$$\alpha(t) = \frac{\pi}{4} - \kappa(t) \quad (\text{B.19})$$

$$\tan[\kappa(t)] = \frac{\Omega_2(t)}{2J_1} + \frac{\Omega_3(t)}{2J}. \quad (\text{B.20})$$

References

- [1] Paul Benioff, J. Stat. Phys. 22, 563 (1980).
- [2] R. Feynman, Int. J. Theo. Phys. 21, 467 (1982).
- [3] S. Lloyd, Science 261, 1569 (1993).
- [4] Y. S. Weinstein, S. Lloyd, and D. G. Cory, Phys. Rev. Lett. 86, 1889 (2001).

- [5] M. A. Nielsen and I. L. Chuang, *Quantum Computation and Quantum Information* (Cambridge University Press, 2000).
- [6] P. W. Shor, *SIAM J. Sci. Statist. Comput.* 26, 1484 (1997).
- [7] L. Ruiz-Perez and J. C. Garcia-Escartin, *Qua. Inf. Process.* 16, 152 (2017).
- [8] S. A. Daniel and S. Lloyd, *Phys. Rev. Lett.* 83, 5162 (1999).
- [9] G. Brassard, P. Hoyer, M. Mosca, and A. Tapp, *Contemp. Math.* 305, 53 (2002).
- [10] P. J. Davis, *Circulant Matrices* (Wiley, New York, 1970).
- [11] Robert M. Gray, *Found. Trends Commun. Inf. Theory* 2, 155 (2006).
- [12] G. Dzhelepov, I. Dokuzova, and D. Razpopov, *Plovdiv Univ. Paisii Khilendarski Nauchn. Trud. Mat.* 38, 17 (2011).
- [13] X. Y. Jiang and K. Hong, Explicit Determinants of the k-Fibonacci and k-Lucas RSFPLR Circulant Matrix in Codes. In: Y. Yang, M. Ma, and B. Liu, (eds) *Information Computing and Applications (ICICA 2013)*. *Communications in Computer and Information Science* (Springer, Berlin, Heidelberg, 2013, vol 391), https://doi.org/10.1007/978-3-642-53932-9_61.
- [14] M. Muzychuk, *Proc. London Math. Soc.* 88, 1 (2004).
- [15] B. Olson, S. Shaw, C. Shi, C. Pierre, and R. G. Parker, *Appl. Mech. Rev.* 66, 040803 (2014).
- [16] D. Razpopov, Four-dimensional Riemannian manifolds with two circulant structures. In: *Mathematics Education Mathematics, Proceedings of 44-th Spring Conference of UBM, SOK Kamchia, Bulgaria*, vol. 44, pp. 179–185 (2015).
- [17] R. M. Roth and A. Lempel, *IEEE Trans. Inform. Theory* 36, 1157 (1990).
- [18] S. S. Zhou, T. Loke, J. A. Izaac, and J. B. Wang, *Qua. Inf. Process.* 16, 82 (2017).
- [19] F. R. Gantmacher, *Matrix Theory* (Springer, Berlin, 1986).
- [20] P. A. Ivanov and N. V. Vitanov, *Sci. Rep.* 10, 5030 (2020).
- [21] H. Wu, X. Huang, C. Hu, Z. Yang, and S. Zheng, *Phys. Rev. A* 96, 022321 (2017).
- [22] D. Guéry-Odelin, A. Ruschhaupt, A. Kiely, E. Torrontegui, S. Martínez-Garaot, and J.-G. Muga, *Rev. Mod. Phys.* 91, 045001 (2019).
- [23] A. Rueda, W. Hease, S. Barzanjeh, and J. M. Fink, *npj Quantum Information* 5, 108 (2019).
- [24] R. Hablützel, *Nonlinear Quantum Optics and Thermodynamics with Three Trapped Ions* (Thesis, National University of Singapore 2018).
- [25] J. K. Pachos, *Int. J. Quan. Inf.* 4, 541 (2006).
- [26] T. Hatomura, *J. Phys. Soc. Jpn.* 86, 094002 (2017).

- [27] M. Born and V. A. Fock, *Zeitschrift für Physik A*. 51, 165 (1928).
- [28] M. V Berry, *Proc. R. Soc. Lond. A* 392, 45 (1984).
- [29] Michael R. Hush, Weibin Li, Sam Genway, Igor Lesanovsky, and Andrew D. Armour, *Phys. Rev. A* 91, 061401(R) (2015).
- [30] K. Kim, M.-S. Chang, R. Islam, S. Korenblit, L.-M. Duan, and C. Monroe, *Phys. Rev. Lett.* 103, 120502 (2009).
- [31] S. X. Wang, *Quantum Gates, Sensors, and Systems with Trapped Ions* (Thesis, Massachusetts Institute of Technology 2012).
- [32] Shiqian Ding, Gleb Maslennikov, Roland Häublützel, and Dzmitry Matsukevich, *Phys. Rev. Lett.* 121, 130502 (2018).
- [33] Easwar Magesan, Robin Blume-Kohout, and Joseph Emerson, *Phys. Rev. A* 84, 012309 (2011).
- [34] C. J. Ballance, T. P. Harty, N. M. Linke, M. A. Sepiol, and D. M. Lucas, *Phys. Rev. Lett.* 117, 060504 (2016).
- [35] J. P. Gaebler, T. R. Tan, Y. Lin, Y. Wan, R. Bowler, A. C. Keith, S. Glancy, K. Coakley, E. Knill, D. Leibfried, and D. J. Wineland, *Phys. Rev. Lett.* 117, 060505 (2016).
- [36] Yukai Wu, Sheng-Tao Wang, and L.-M. Duan, *Phys. Rev. A* 97, 062325 (2018).
- [37] Armin Uhlmann, *Phys. Rev. A* 62, 032307 (2000).
- [38] Xi Chen, I. Lizuain, A. Ruschhaupt, D. Guéry-Odelin, and J. G. Muga, *Phys. Rev. Lett.* 105, 123003 (2010).